Processing and Application of Ceramics 10 [4] (2016) 249–256
DOI: 10.2298/PAC1604249M

Preparation of nanocrystalline composite TiO_2-SnO_2 powders using sol-gel method combined with hydrothermal treatment

Anna Marzec[1,*], Zbigniew Pędzich[1], Wojciech Maziarz[2]

[1]*AGH - University of Science and Technology, Faculty of Materials Science and Ceramics, Department of Ceramics and Refractory Materials, Mickiewicza 30, 30-059 Krakow, Poland*
[2]*Institute of Metallurgy and Materials Science of Polish Academy of Sciences, Reymonta 25, 30-059 Krakow, Poland*

Received 31 August 2016; Received in revised form 21 October 2016; Accepted 21 November 2016

Abstract

The paper describes the process of TiO_2-SnO_2 nanocomposites manufacturing utilizing two-step sol-gel method combined with calcination (in the case of titanium hydroxide gel) or hydrothermal treatment (in the case of tin hydroxide). Phase composition of the obtained nanopowders and average crystallite sizes were determined using XRD analysis. Measurements of the specific surface area were performed using sorption method based on determination of physical adsorption isotherm (BET). Morphology of the nanopowders was observed using transmission electron microscope. The presented synthesis method enables to obtain composites nanopowders from TiO_2-SnO_2 system with known and controlled chemical and phase compositions, and distinctly diversified TiO_2 and SnO_2 particle sizes.

Keywords: *nanocomposites TiO_2-SnO_2, nanopowders, sol-gel method, hydrothermal treatment*

I. Introduction

Nanocomposites based on TiO_2 and SnO_2 are widely used in nanoelectronics, heterogeneous photocatalysis or optoelectronics, but the main area of the usage of TiO_2-SnO_2 composite materials is chemical sensors manufacturing. TiO_2-SnO_2 sensors are characterized by high sensitivity and high selectivity thanks to the ability to modify of electron structure, which is a result of interaction between two components. A direct connection between grains results in incurvation of bands, and the observed transfer of charges from TiO_2 to SnO_2 is caused by difference in valence band and bandwidth [1–3].

Different methods were used to obtain composites TiO_2-SnO_2 nanopowders. One of them is the flame synthesis that enables preparation of composites on nanoscale with different oxide mass fraction [4]. Other methods, which provide the possibility to produce this type of material, are pyrolysis and mechanical synthesis. However, these methods do not enable control of the particle size and their mutual spatial distribution, as well as phase composition [5,6]. Two-stage synthesis method of nanocomposites combined in case of titanium hydroxide gel with calcination, and in case of tin hydroxide with hydrothermal treatment creates a unique possibility to control crystallites size and microstructure arrangement of both types of grains which compose the material. During the synthesis, admixtures are built into the crystal lattice uniformly, because there is practically no diffusion at temperature of the process, and therefore admixture neither agglomerates nor segregates [7,8]. Two-stage synthesis seems to be the most beneficial method due to the possibilities to control the morphology of nanocomposites as well as low costs of production [9,10].

The work presents physicochemical and structural characterization of composite TiO_2-SnO_2 nanopowders produced by multiplex sol-gel method combined with hydrothermal treatment of obtained hydroxide gel.

II. Materials and methods

2.1. Samples preparation

Nanocomposites in the TiO_2-SnO_2 system were obtained with multiplex, modified sol-gel method. In the

* Corresponding author: tel: +48 12 617 24 96,
fax: +48 12 633 46 30, e-mail: *amarzec@agh.edu.pl*

first step, nanocrystalline TiO_2, which subsequently was used for preparation of nanocomposites powders, was synthesized by sol-gel method. The procedure for obtaining TiO_2 consisted of instilling each time 20 cm^3 of titanium (IV) isopropanol (98%) to 200 cm^3 of isopropyl alcohol, which has been set to pH~3 using HCl (36%) and CH_3COOH (27%) in a volume ratio of 1:10. The obtained solution was stirred for 30 minutes at room temperature, and then poured to 160 cm^3 of distilled water and intensively stirred for 1 hour at room temperature. The obtained gels were dried at 115 °C for 18 hours and calcined for 2 hours at 400, 450, 500, 540 or 560 °C (the samples denoted T-1, T-2, T-3, T-4 and T-5, respectively). Calcination temperature selection depends on the size of the obtained TiO_2 particles, phase composition (anatase/rutile), as well as the degree of agglomeration. Finally, the obtained TiO_2 powders were ground in mortar.

Subsequently, in order to obtain TiO_2-SnO_2 nanocomposites with different SnO_2 mass fraction containing TiO_2 nanoparticles with the average size of ~30 nm (e.g. 26.9, 44.1 and 74.0 wt.% SnO_2 – the samples denoted TS-1, TS-2 and TS-3, respectively), TiO_2 powder prepared by calcination of the titanium hydroxide gel at 540 °C was used. SnO_2 nanoparticles were introduced into the composition by hydrothermal treatment of hydroxide gel. For that purpose, in the first step a colloidal solution was prepared by ultrasonically dispersing 2 g of the selected TiO_2 nanopowder in NH_4OH-water solution (60 cm^3 NH_4OH 25% was dissolved in 160 cm^3 of distilled water) under constant stirring conditions. In the next step each time appropriate amount of $SnCl_4$ precursor (99%) was diluted ten times in distilled water at room temperature and instilled to the prepared colloidal solution. Then the suspensions were transferred to Teflon vessels and placed in a reactor. Crystallization process at hydrothermal conditions was conducted in three-temperature cycle (195 min at 160 °C, 60 min at 170 °C and 1350 min at 180 °C) under constant stirring conditions (100 rpm). Upon completion of hydrothermal crystallization process, the suspensions were washed repeatedly with distilled water, filtered and dried to the constant mass in the laboratory dryer at 115 °C. Finally, the dried powders were ground in a mortar.

2.2. Characterization

Calcination temperature of titanium hydroxide gel was determined based on TG/DSC analysis carried out using Netzsch STA 409 equipment.

In order to determine the phase composition of the obtained nanopowders, powder X-ray diffraction (XRD) method was applied using X'Pert Pro PANalytical Company apparatus, running in the Bragg-Brentano configuration, with 2θ angle ranging from 10° to 70° with step size of 0.008°. With XRD technique an average size of TiO_2 crystallites was also determined using Scherrer formula.

Measurements of powders specific surface area were conducted with sorption method based on measurements of physical adsorption isotherm (BET). The amount of adsorbed gaseous nitrogen at −196 °C on powders surfaces was detected. Powdered samples with mass of about 0.2 g were subjected to degassing at 110 °C for 3 h. Adsorption measurements were conducted in relative pressures (p/p_s) ranging from 0.01 to 1 and the specific surfaces area was determined by BET method. Measurements were conducted using Novelties 1200e Quantachrome Instruments Company device.

In order to determine the morphology of the obtained composite TiO_2-SnO_2 nanopowders the high resolution transmission electron microscope (TEM, TECNAI FEG of FEI Company) with accelerating voltage of 200 kV was used. This microscope was also used to determine the actual position of atoms on the images in dark visual field obtained with scanning-transmission technique STEM-HAADF connected with EDS microanalysis, which enabled identification of chemical elements included in the studied materials.

III. Results and discussion

3.1. Characterization of TiO_2 nanopowder

Calcination temperature of titanium hydroxide was based on the results of TG/DSC analysis, which was carried out for titanium hydroxide gel (Fig. 1). On the TG curve two distinct weight loss intervals of different size may be specified. The first (loss of 13.41 wt.%) up to ~250 °C is related to loss of excessive amounts of water and the occluded solvent. On the DSC curve weak endothermic peaks are visible within the discussed range of temperature. The second interval of weight loss (7.08 wt.%) occurs at temperature ranging from 250 to 400 °C. The exothermic peaks at 257.9 °C and 342.5 °C on the DCS curve result from the combustion of organic compounds used for TiO_2 production. Another change in enthalpy on the DSC curve may be related to the phase transition of TiO_2 anatase into rutile at 593.4 °C.

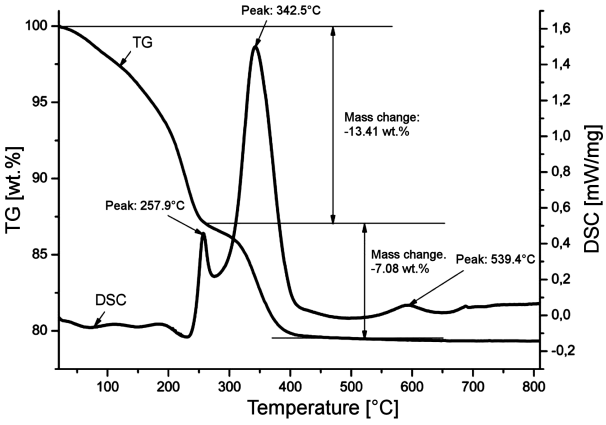

Figure 1. Results of TG/DSC analysis of the initial titanium hydroxide gel

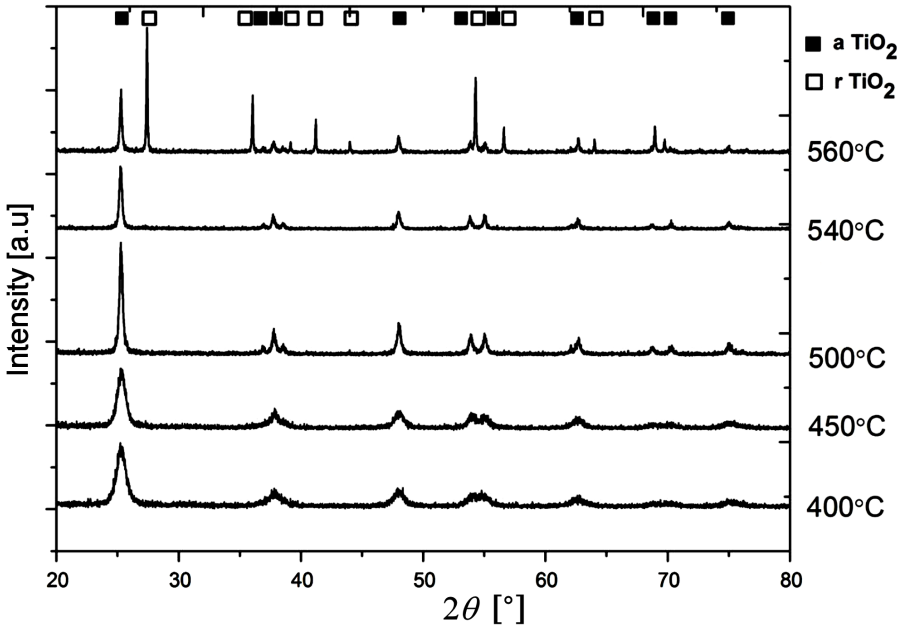

Figure 2. XRD diffractograms of the synthesized nanopowders calcined at different temperatures

Phase composition of the obtained nanopowders (Fig. 2) and average crystallite sizes were determined with X-ray diffraction technique. Titanium (IV) oxide crystallizes at 400 °C in tetragonal anatase structure. Along with an increase in calcination temperature, the size of crystallites increases, but the phase composition of the nanopowders remains unchanged. However, on the diffractogram of the sample T-5 calcined at 560 °C it is possible to observe peaks of stable rutile structure together with peaks of the anatase structure. The average crystallite sizes and mass fraction of both titania phases were estimated from XRD patterns and presented in Table 1.

Table 1 also presents measured values of the BET specific surface area and estimated average particle sizes of the powders. Specific surface of the sample T-1 calcined at 400 °C is the highest (119.8 m^2/g), and the average sizes of anatase particles obtained at this temperature was estimated to be 13.2 nm. The calcined powders at 560 °C are characterized with the lower specific surface area of 24.2 m^2/g.

The powder T-4 calcined at 540 °C with the largest anatase crystallites was selected for synthesis of the composite TiO_2-SnO_2 samples. Microscopic observations of the TiO_2 T-4 powder were carried out using transmission electron microscope and presented in Fig. 3. Based on these observations, it was found that the obtained powder is characterized by some degree of agglomeration. However, the formed aggregations are quite loose, so single grains show crystallite size similar to that calculated by XRD technique.

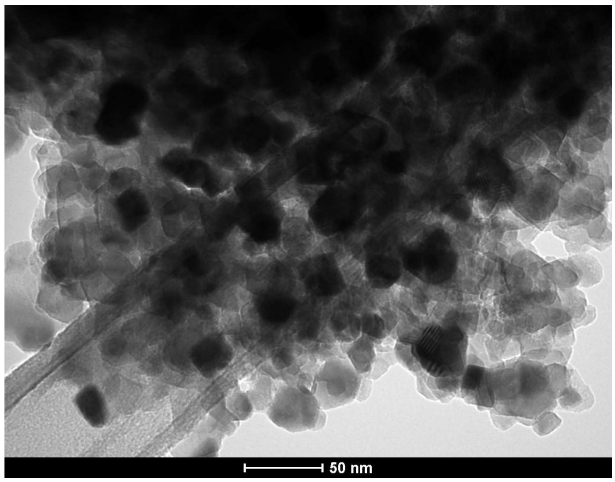

Figure 3. TEM microphotographs of TiO_2 nanopowder (sample T-4)

In order to examine the chemical composition of the

Table 1. Selected properties of investigated titanium powders: mass fractions of titania phases (a TiO_2 - anatase, r TiO_2 - rutile), average crystallite size from XRD (D_{hkl}), specific surface area (SSA) and estimated particle size from BET (D_{BET})

Sample	Calcination temperature [°C]	Amount of titania phases [wt.%]	D_{hkl} [nm]	SSA [m^2/g]	D_{BET} [nm]
T-1	400	a TiO_2 - 100%	a TiO_2 - 8.0 ± 0.2	119.8 ± 5.2	13.2 ± 1.2
T-2	450	a TiO_2 - 100%	a TiO_2 - 10.2 ± 0.2	108.3 ± 5.2	14.6 ± 1.2
T-3	500	a TiO_2 - 100%	a TiO_2 - 25.1 ± 0.2	42.1 ± 5.2	37.5 ± 1.2
T-4	540	a TiO_2 - 100%	a TiO_2 - 33.8 ± 0.2	36.0 ± 5.2	43.9 ± 1.2
T-5	560	a TiO_2 - 40,2% r TiO_2 - 59,8%	a TiO_2 - 46.0 ± 0.2 r TiO_2 - 146.0 ± 0.2	24.2 ± 5.2	-

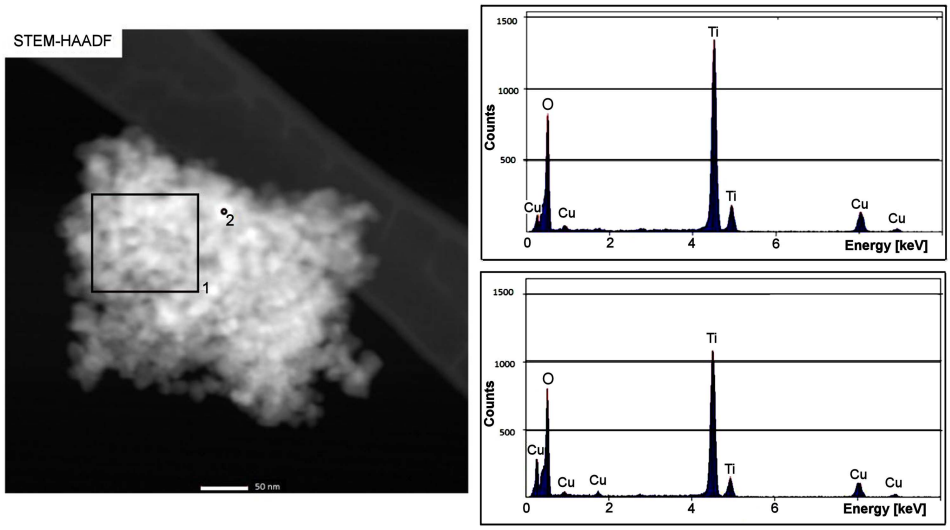

Figure 4. STEM-HAADF images of TiO_2 powder T-4 with EDS spectrum of the selected area (1) and point (2)

TiO_2 T-4 powder, the EDS analysis was carried out. EDS spectra of the sample T-4 from the marked surface and point, as well as STEM-HAADF image were presented in Fig. 4. EDS analyses confirmed the chemical composition of sample and presence of Ti and O.

High resolution transmission electron microscopy HRTEM was also used to observe the crystal structure of the TiO_2 T-4 powder. By analyzing the distribution of atomic plains, single TiO_2 units were recognized.

Figure 4 shows HRTEM of the T-4 powder along with Fourier transform from marked surface. Atomic plains are visible on the image with emphasized values of interlayer spacing. By analysing their values, it was found that the crystalline anatase was located in marked surface in Fig. 5. Values of interlayer spacing for crystallographic orientation of (111) anatase is d_{111} = 3.6 Å.

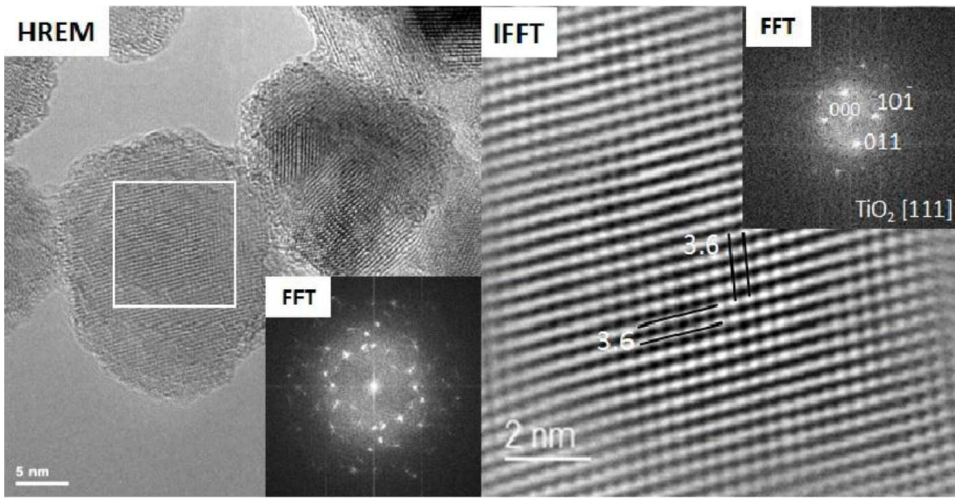

Figure 5. HRTEM images of TiO_2 powder (sample T-4)

Table 2. Selected properties of investigated composite powders: mass fractions of phases (a TiO_2 - anatase, k SnO_2 - cassiterite), average crystallite size from XRD (D_{hkl}), specific surface area (SSA) and estimated particle size from BET (D_{BET})

Sample	Amount of phases [wt.%]	D_{hkl} [nm]	SSA [m^2/g]	D_{BET} [nm]
T-4	a TiO_2 100% k SnO_2 0%	a TiO_2 33.8 ± 0.2	36.0 ± 5.2	43.9 ± 1.2
TS-1	a TiO_2 73.1% k SnO_2 26.9%	a TiO_2 35.0 ± 0.2 k SnO_2 3.7 ± 0.2	69.5 ± 5.2	
TS-2	a TiO_2 55.9% k SnO_2 44.1%	a TiO_2 30.2 ± 0.2 k SnO_2 3.6 ± 0.2	92.1 ± 5.2	
TS-3	a TiO_2 26.0% k SnO_2 74.0%	a TiO_2 30.2 ± 0.2 k SnO_2 3.6 ± 0.2	136.3 ± 5.2	

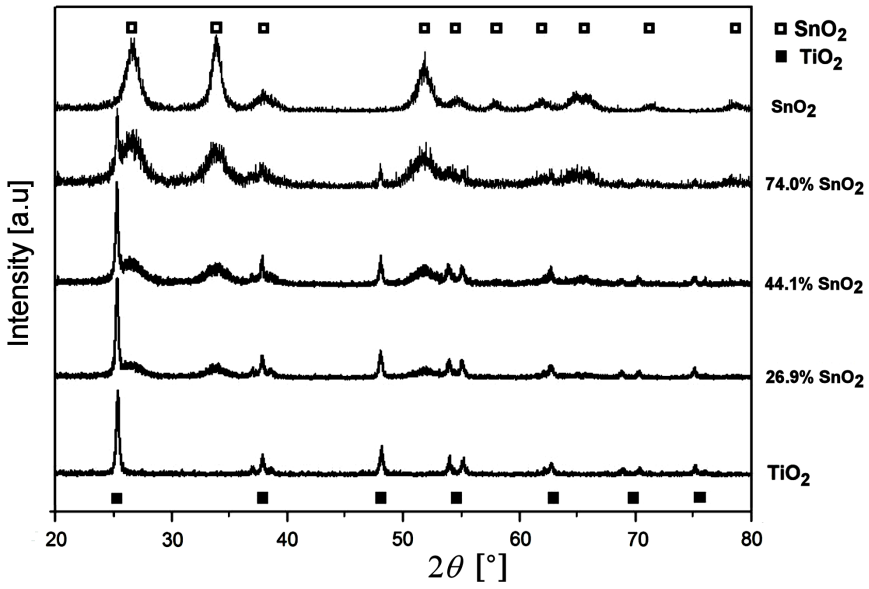

Figure 6. XRD diffractograms of the synthesized TiO_2-SnO_2 nanocomposites

3.2. Characterization of TiO_2-SnO_2 nanocomposites

Phase composition of the obtained TiO_2-SnO_2 nanocomposites with TiO_2 particles sizes of about 30 nm and different SnO_2 mass fraction (26.9, 44.1 and 74.0 wt.%) was determined using XRD method (Fig. 6). Diffractograms for TiO_2 and SnO_2 powders are also presented for comparison. Titanium dioxide occurs in thermodynamically stable, tetragonal, anatase structure. For tin dioxide there are also visible reflections only from tetragonal, cassiterite structure. Mass fraction of both oxides and average crystallite sizes were presented in Table 2.

Table 2 also presents values of the specific surface area determined by BET method. The value of specific surface area of the TiO_2 T-4 powder obtained by calcination at 540 °C is the lowest one (36.0 m^2/g). Along with the increase of SnO_2 content, in the composite the value of specific surface area increases, as a result of rise of the particle number with a smaller size.

In order to determine the morphology of nanocomposites, their microscopic observation was carried out using TEM (Fig. 7–9). TEM results showed the presence of grains diversified in terms of size. A few nanometric SnO_2 grains were located on the surface of

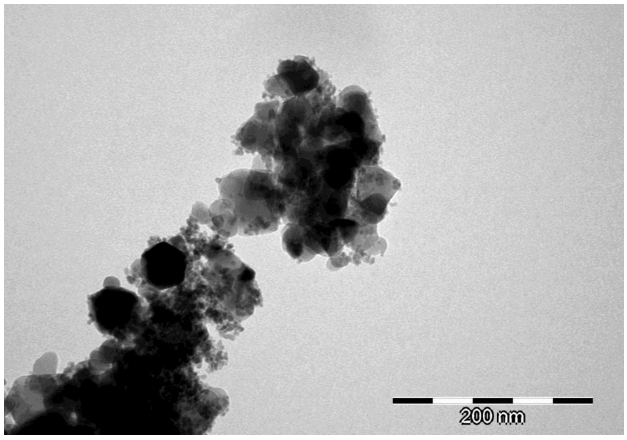

Figure 7. TEM microphotographs of the composite powder containing 26.9 wt.% SnO_2

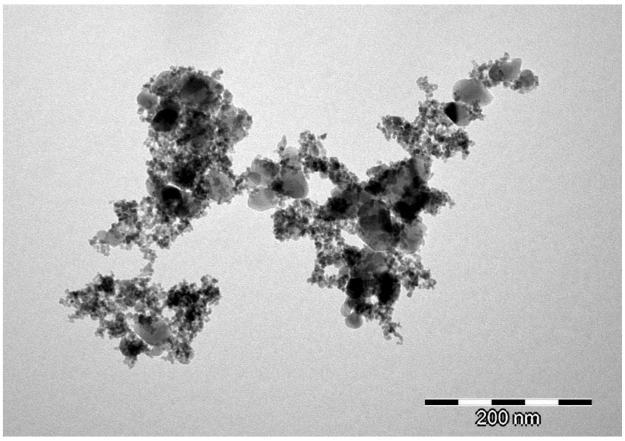

Figure 8. TEM microphotographs of the composite powder containing 44.1 wt.% SnO_2

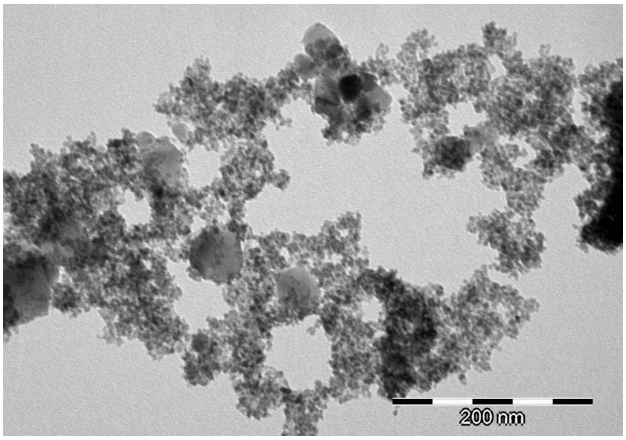

Figure 9. TEM microphotographs of the composite powder containing 74.0 wt.% SnO_2

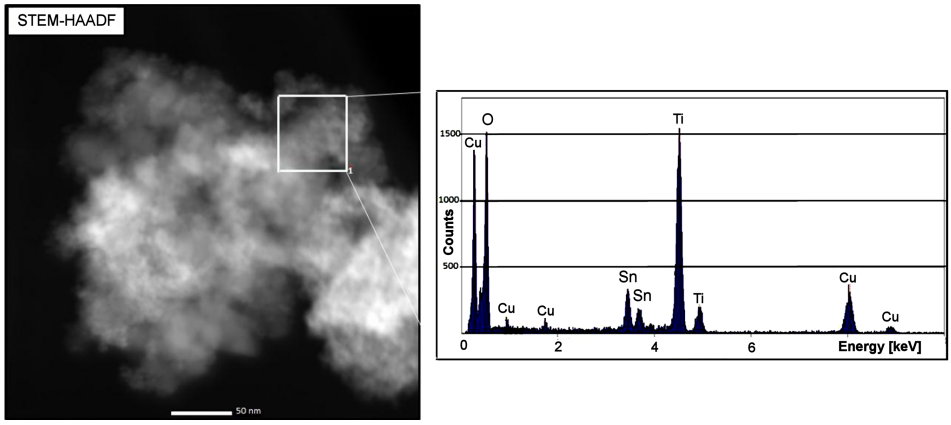

Figure 10. STEM-HAADF images of composite powder containing 44.1 wt.% SnO_2 with EDS spectrum of the selected area

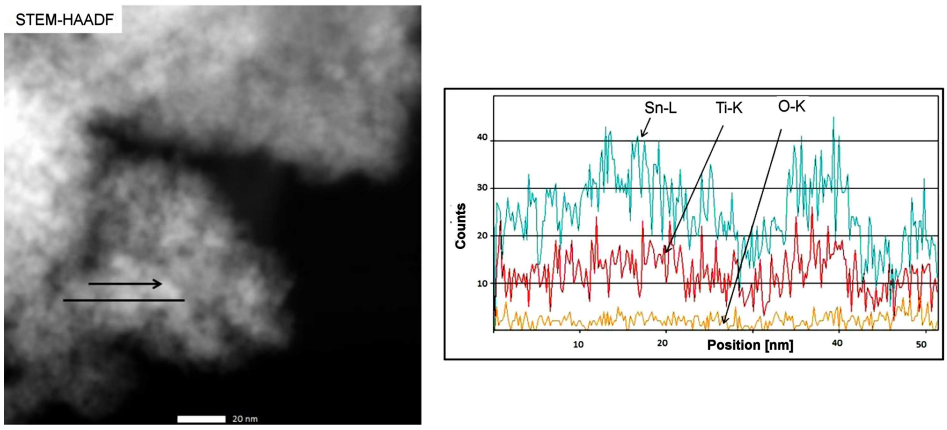

Figure 11. STEM-HAADF images of composite powder containing 44.1 wt.% SnO_2 with EDS spectrum of the linear analysis

several nanometric poorly agglomerated TiO_2 grains. Grains distribution is diversified and varies along with the composition of nanopowders. In the nanocomposites containing smaller amount of SnO_2 (26.9 and 44.1 wt.%), cassiterite nanoparticles are settled on the surface of anatase grains. Along with the increase of SnO_2 content in the composites higher degree of agglomeration was observed due to the higher surface area, and thus large surface energy. However, aggregation of grains is quite loose, so single grains show crystallites size similar to that determined by XRD technique.

In order to identify the elements included in powders, their EDS analysis was carried out. EDS sample spectrum and STEM-HAADF images for composite containing 44.1 wt.% of SnO_2 were presented in Figs. 10 and 11. The examined composite consisted of Ti, Sn and O.

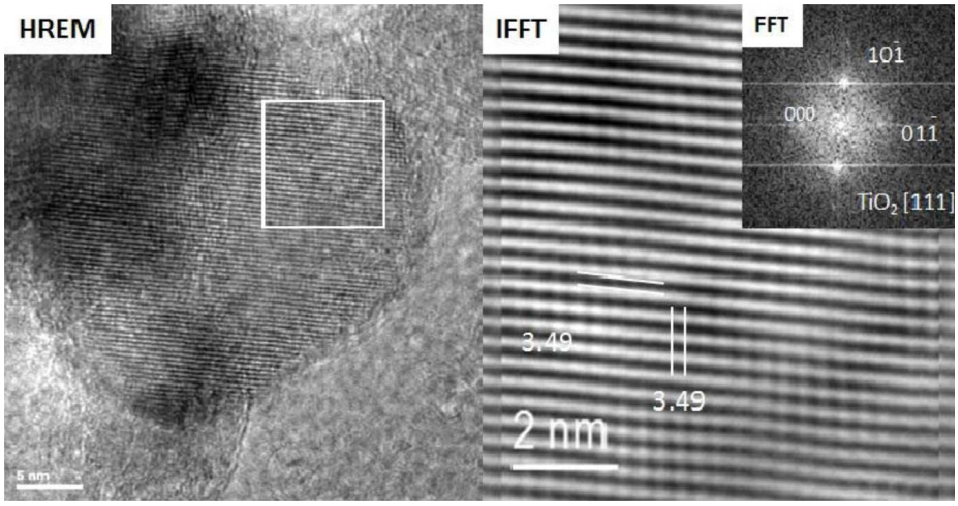

Figure 12. HRTEM images of nanocomposite containing 44.1 wt.% SnO_2 showing crystalline TiO_2 (anatase)

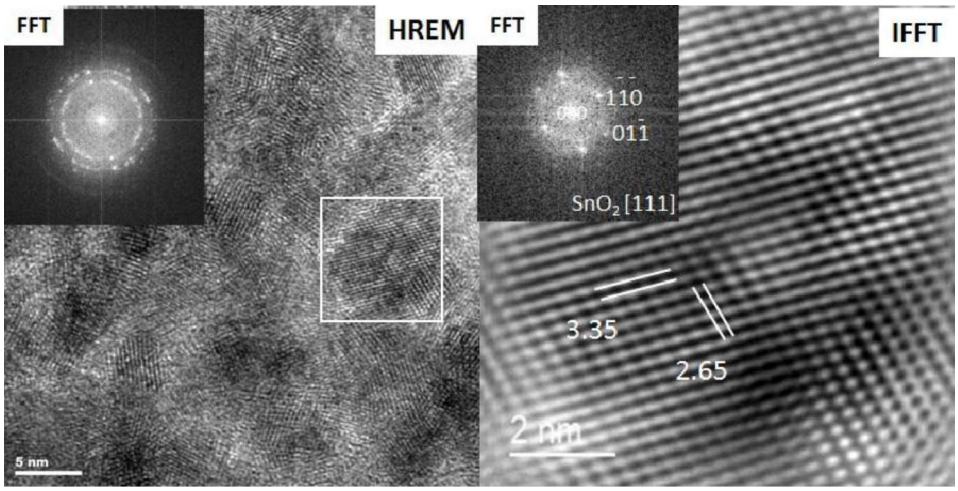

Figure 13. HRTEM images of nanocomposite containing 44.1 wt.% SnO_2 showing crystalline SnO_2 (cassiterite)

HRTEM microscope was also used to observe the structure of the nanocomposite TS-2 containing 44.1 wt.% of SnO_2, Figs. 9 and 10. By analysing individual values of interlayer spacing, single particles in the powder composite were recognized. Figures 12 and 13 show HRTEM micrographs of nanocomposite along with Fourier transform from marked surfaces. Atomic plains with emphasized values of interlayer spacing, characteristic for anatase (Fig. 12) and for cassiterite (Fig. 13) are visible.

IV. Conclusions

Composite TiO_2-SnO_2 nanopowders were produced by multiplex sol-gel method combined with hydrothermal treatment. Presented synthesis method enables synthesis of composites in the TiO_2-SnO_2 system, not only with known and controlled chemical and phase composition, but also with distinct diversified TiO_2 and SnO_2 particle sizes. BET analysis showed that the obtained nanocomposites TiO_2-SnO_2 are characterized by a large specific surface area, which increases along with SnO_2 content in the composite. Based on microscopic TEM observation, it was found that hydrothermal method allows more precise control of the size, phase composition and mutual, spatial distribution of composite elements than methods known so far. As an effect of proposed fabrication procedure the final composite microstructure is not a random mixture of anatase and cassiterite grains but rather larger anatase grains skeleton covered by smaller cassiterite ones. Such composite architecture could be promising for sensor application due to type of conductivity of both phases and their role in charge transfer during work of sensor. The composite nanoparticles consisting of larger anatase grains skeleton covered by smaller cassiterite ones seem to be promising candidates for gas sensor applications.

Acknowledgements: This work was made with financial support of the Polish State Ministry of Science and Higher Education under grant no. AGH 15.11.160.619, the National Science Centre (NCN) based on the decision number DEC-2015/19/N/ST8/00187. Support was also given by the Polish Ceramic Society. The authors thank to Prof. Bućko for executing X-ray diffraction analyses.

References

1. G. Kenanakis, D. Vernardou, E. Koudoumasa, G. Kiriakidis, N. Katsarakis, "Ozone sensing properties of ZnO nanostructures grown by the aqueous chemical growth technique", *Sensors Actuators B*, **124** (2007) 187–190.
2. Y. Shimizu, A. Jono, T. Hyodo, M. Egashira, "Preparation of large mesoporous SnO_2 powder for gas sensor application", *Sensors Actuators B*, **108** (2005) 56–61.
3. B. Renganathan, D. Sastikumar, G. Gobi, N. Rajeswari Yogamalar, A. Chandra Bose, "Nanocrystalline ZnO coated fiber optic sensor for ammonia gas detection", *Optics Laser Technol.*, **43** (2011) 1398–1404.
4. K.K. Akurati, A. Vital, R. Hany, B. Bommer, T. Graule, M. Winterer, "One-step flame synthesis of SnO_2/TiO_2 composite nanoparticles for photocatalytic applications", *Int. J. Photoenergy*, **7** (2005) 153–161.
5. A. Kusior, J. Klich-Kafel, M. Radecka, M. Lubecka, A. Czapla, K. Zakrzewska, "Nanocomposites TiO_2/SnO_2 as resistive gas sensors", *Elektronika*, **2012** [6] (2012) 26–27.
6. P.V. Nho, T.K. Cuong, "Preparation and characterization of nanocomposite TiO_2/SnO_2 films", *VNU J. Sci. Mat. Phys.*, **24** (2008) 42–46.
7. Y. Shimizu, A. Jono, T. Hyodo, M. Egashira, "Preparation of large mesoporous SnO_2 powder for gas sensor application", *Sensors Actuators B*, **108** (2005) 56–61.
8. B. Renganathan, D. Sastikumar, G. Gobi, N. Rajeswari Yogamalar, A. Chandra Bose, "Nanocrystalline ZnO coated fiber optic sensor for ammonia

gas detection", *Optics Laser Technol.*, **43** (2011) 1398–1404.
9. S. Khoby-Shendy, M.R. Vaezi, T. Ebadzadeh, "Synthesis of TiO_2/SnO_2 core shell nanocomposite via sol-gel method", *Int. J. Modern Phys., Conf. Series*, **5** (2012) 251–256.
10. W. Zeng, T. Liu, Z. Wang, "Sensitivity improvement of TiO_2-doped SnO_2 to volatile organic compounds", *Physica E*, **43** (2010) 633–638.
11. A. Marzec, M. Radecka, W. Maziarz, A. Kusior, Z. Pędzich, "Structural, optical and electrical properties of nanocrystalline TiO_2, SnO_2 and their composites obtained by the sol-gel method", *J. Eur. Ceram. Soc.*, **36** (2016) 2981–2989.